

TMCI threshold with space charge and different wake fields

V. Balbekov*

*Fermi National Accelerator Laboratory
P.O. Box 500, Batavia,
Illinois 60510, email balbekov@fnal.gov
(Dated: August 23, 2016)*

Transverse mode coupling instability of a bunch with space charge and wake field is considered within the frameworks of the boxcar model. Eigenfunctions of the bunch without wake are used as a basis for the solution of the equations with the wake field included. A dispersion equation for constant wake is presented in the form of an infinite continued fraction and also as the recursive relation with an arbitrary number of the basis functions. Realistic wake fields are considered as well including resistive wall, square, and oscillating wakes. It is shown that the TMCI threshold of the negative wake grows up in absolute value when the SC tune shift increases. Threshold of positive wake goes down at the increasing SC tune shift. The explanation is developed by an analysis of the bunch spectrum.

PACS numbers: 29.27.Bd

I. INTRODUCTION

Transverse mode coupling instability (TMCI) has been observed first in PETRA and explained by Kohaupt on the base of the two-particle model [1]. A lot of papers on this subject have been published later, including handbooks and surveys (see e.g. [2]). It is established that the instability occurs as a result of a coalescence of the neighboring head-tail tunes caused by the bunch wake field.

TMCI with space charge has been considered first by Blaskiewicz [3]. The main point of this paper is that the SC pushes up the TMCI threshold that improves the beam stability. However, a non-monotonic dependence of the TMCI threshold and rate on the SC tune shift has been sometimes demonstrated in the paper. It was following from several examples that the stability and instability areas can change each other when the tune shift increases. The results have been confirmed later by the same author with help of numerical simulation of the instability at modest magnitude of the SC tune shift [4]

So-termed three-mode model has been developed in Ref. [7] for analytical description of the TMCI with space charge, chromaticity, and arbitrary wake. This simple model confirms that the TMCI threshold of negative wakes goes up in modulus when the SC tune shift increases. However, only the case of modest SC has been investigated in [7] though the proposed equations allow to suggest that a sudden kink of the threshold curve is possible at the higher shift. Therefore, field of application of the three-mode model is still an open question.

The case of very high space charge has been considered in Ref. [5, 6] It was confirmed in both papers that the space charge heightens the TMCI threshold until the ratio of the SC tunes shift to synchrotron tune is less of

several tens or a hundred. However, the authors have expressed the different opinions about further behavior of the threshold. As it follows from [6], the threshold growth should continue at higher SC as well. On the contrary, it was suggested in Ref. [5] that the threshold growth can cease and turn back over the mention boundary.

The last statement has been supported in my recent preprint [8]. I have used the known eigenfunctions of the boxcar bunch [9] to get a convenient basis for investigation of the TMCI problem in depth. However, disclosure of some errors at numerical solutions of obtained equations forces me to revise the conclusions. The equations are recomputed in presented paper at any value of the SC tune shift and different wakes including the resistive wall, square, the oscillating ones. The pushing up of the TMCI threshold by the SC is observed in all the cases.

II. BASIC EQUATIONS AND ASSUMPTIONS

The terms, basic symbols and equations of Ref. [7] are used in this paper. In particular, linear synchrotron oscillations are considered here being characterized by amplitude A and phase ϕ , or by corresponding Cartesian coordinates:

$$\theta = A \cos \phi, \quad u = A \sin \phi. \quad (1)$$

Thus θ is the azimuthal deviation of a particle from the bunch center in the rest frame, and variable u is proportional to the momentum deviation about the bunch central momentum (the proportionality coefficient plays no part in the paper). Transverse coherent displacement of the particles in some point of the longitudinal phase space will be presented as real part of the function

$$X(A, \phi, t) = Y(A, \phi) \exp \left[-i(Q_0 + \zeta) \theta - i(Q_0 + \nu) \Omega_0 t \right] \quad (2)$$

where Ω_0 is the revolution frequency, Q_0 is the central betatron tune, and ν is the tune addition produced by

*Electronic address: balbekov@fnal.gov

space charge and wake field. Generally, ζ is the normalized chromaticity, however, only the case $\zeta = 0$ will be investigated in this paper. Then the function Y satisfies the equation [6],[7]:

$$\begin{aligned} \nu Y + i Q_s \frac{\partial Y}{\partial \phi} + \Delta Q(\theta) [Y(\theta, u) - \bar{Y}(\theta)] \\ = 2 \int_{\theta}^{\infty} q(\theta' - \theta) \bar{Y}(\theta') \rho(\theta') d\theta' \end{aligned} \quad (3)$$

where $F(\theta, u)$ and $\rho(\theta)$ are the normalized distribution function and corresponding linear density of the bunch, Q_s is the synchrotron tune, $\Delta Q(\theta) \propto \rho(\theta)$ is the space charge tune shift, and $\bar{Y}(\theta)$ is the bunch displacement in usual space which can be found by the formula

$$\rho(\theta) \bar{Y}(\theta) = \int_{-\infty}^{\infty} F(\theta, u) Y(\theta, u) du. \quad (4)$$

The function $q(\theta)$ is proportional to the usual transverse wake field W_1

$$q = \frac{r_0 R N_b W_1}{8\pi\beta\gamma Q_0} \quad (5)$$

with $r_0 = e^2/mc^2$ as classic radius of the particle, R as the accelerator radius, N_b as the bunch population, β and γ as the normalized velocity and energy [2].

A solution of Eq. (3) can be found by its expansion in terms of the eigenfunctions of corresponding homogeneous equation which is

$$\nu_j Y_j + i Q_s \frac{\partial Y_j}{\partial \phi} + \Delta Q(\theta) [Y_j(\theta, u) - \bar{Y}_j(\theta)] = 0. \quad (6)$$

It is easy to check that the functions form an orthogonal basis with the weighting function $F(\theta, u)$. Besides, we will impose the normalization condition:

$$\int \int F(\theta, u) Y_j^*(\theta, u) Y_k(\theta, u) d\theta du = \delta_{jk} \quad (7)$$

where the star means complex conjugation. Then, looking for the solution of Eq. (3) in the form

$$Y = \sum_j C_j Y_j, \quad (8)$$

one can get the expression for the unknown coefficients C_j :

$$\sum_j (\nu - \nu_j) C_j Y_j = 2 \sum_j C_j \int_{\theta}^{\infty} \bar{Y}_j(\theta') \rho(\theta') q(\theta' - \theta) d\theta' \quad (9)$$

where \bar{Y}_j and Y_j are also connected by Eq. (4). Multiplying Eq. (9) by factor $F(\theta, u) Y_j^*(\theta, u)$, integrating over θ and u , and using normalization condition (7) one can get the series of equations for the coefficients C_j :

$$\begin{aligned} (\nu - \nu_j) C_j = 2 \sum_j C_j \int_{-\infty}^{\infty} \rho(\theta) \bar{Y}_j^*(\theta) d\theta \\ \times \int_{\theta}^{\infty} \rho(\theta') \bar{Y}_j(\theta') q(\theta' - \theta) d\theta'. \end{aligned} \quad (10)$$

III. BOXCAR MODEL

The boxcar model is characterized by following expressions for the bunch distribution function and its linear density:

$$F = \frac{1}{2\pi\sqrt{1-A^2}} = \frac{1}{2\pi\sqrt{1-\theta^2-u^2}}, \quad (11a)$$

$$\rho(\theta) = \frac{1}{2} \quad \text{at} \quad |\theta| < 1. \quad (11b)$$

Because the eigenfunctions depend on two variables (θ, u) (or $A-\phi$), it is more convenient to represent j as a pair of the indexes:

$$j \equiv \{n, m\}, \quad Y_j \equiv Y_{n,m}. \quad (12)$$

An analytical solutions of Eq. (6) for the boxcar bunch have been found by Sacherer [9]. The most important point is that the averaged eigenfunctions $\bar{Y}_{n,m}$ do not depend on second index being proportional to the Legendre polynomials: $\bar{Y}_{n,m}(\theta) \propto 2\bar{Y}_n(\theta) \propto P_n(\theta)$, $n = 0, 1, 2, \dots$. At any n , there are $n+1$ different eigenmodes $Y_{n,m}(\theta, u)$ satisfying the equation

$$(\nu_{n,m} + \Delta Q) Y_{n,m} + i Q_s \frac{\partial Y_{n,m}}{\partial \phi} = \Delta Q S_{n,m} P_n(\theta) \quad (13)$$

where $m = n, n-2, \dots, -n$. The space charge tune shift ΔQ is constant in this model, and the coefficients $S_{n,m}$ are added to the right-hand part of the equation to meet the normalization condition given by Eq. (7). Details of these calculations are placed in the Appendix, and several important examples are represented in Figs. 1 and 2. Dependence of the eigentunes on the SC tune shift is shown in Fig. 1. It is seen that all of them take start at $\Delta Q = 0$ from the points $\nu_{n,m}(0) = mQ_s$. It is the commonly accepted convention to use the term ‘‘multipole’’ for the collective synchrotron oscillations of such frequency, that is the index m should be treated here as the multipole number. Another index n characterizes the eigenfunction power. This feature is normally associated with a radial mode number, the lower power corresponding to the lower number. Because $n \geq |m|$ in this case, the mode $\{m, m\}$ should be treated as the lowest radial mode of m -th multipole.

At $\Delta Q \neq 0$, the multipoles mix together, and the eigentunes split on 2 groups. In the first of them, all tunes have positive value which tends to 0 at $\Delta Q/Q_s \rightarrow \infty$. By the origin, all of them are the lowest radial modes $\{n, n\}$. Corresponding normalizing coefficients $S_{m,m}^2 \rightarrow 2n+1$ at $\Delta Q/Q_s \rightarrow \infty$ (Fig. 2). In second group, the tunes are about $\nu_{n,m} \simeq mQ_s - \Delta Q$ being weakly dependent on the radial index n . The normalizing coefficients tend to 0 in this group.

Note that the transient conjugations of some eigentunes (the line crossing in Fig. 1) is not an evidence of

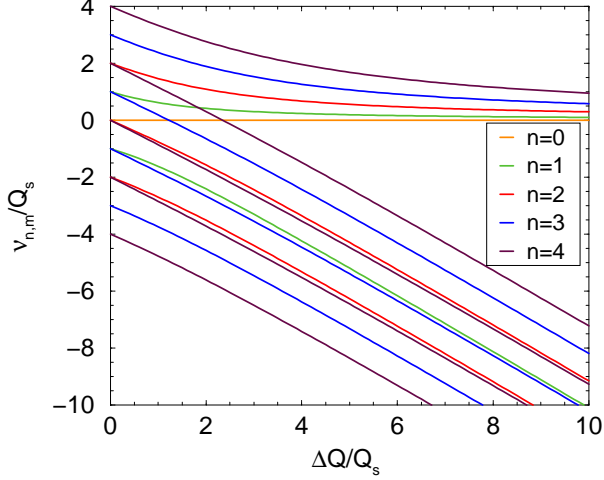


FIG. 1: Eigentunes of the boxcar bunch without wake. At any n , there are $n + 1$ eigentunes starting at $\Delta Q = 0$ from the points $\nu_{n,m} = mQ_s$, $m = n, n-2, \dots, -n$.

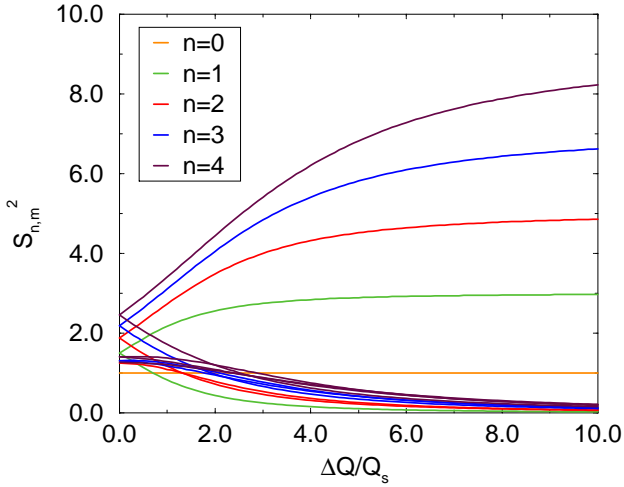


FIG. 2: Normalizing coefficients of the boxcar bunch. The rising lines refer to the case $m = n$.

instability in the case, because corresponding eigenfunctions are orthogonal and uncoupled.

With $\tilde{Y}_{n,m} = S_{n,m}P_n(\theta)$, series (10) for the boxcar bunch obtains the form

$$(\nu - \nu_{N,M})C_{N,M} = q_0 S_{N,M}^* \sum_{n=0}^{\infty} R_{N,n} \sum_m S_{n,m} C_{n,m} \quad (14)$$

with the matrix

$$R_{N,n} = \frac{1}{2} \int_{-1}^1 P_N(\theta) d\theta \int_{\theta}^1 P_n(\theta') w(\theta' - \theta) d\theta'. \quad (15)$$

The notation

$$q(\theta) = q_0 w(\theta) \quad (16)$$

is used here and later to separate the wake strength from its form, and to get the relation

$$R_{0,0} = \frac{1}{2} \int_0^2 (2 - \theta) w(\theta) d\theta = 1. \quad (17)$$

Besides we will use the designations

$$Z_n = \sum_m S_{n,m} C_{n,m}, \quad (18a)$$

$$W_n(\nu) = \sum_m \frac{|S_{n,m}|^2}{\nu - \nu_{n,m}}. \quad (18b)$$

Then series (14) obtains the most compact form

$$Z_N = q_0 W_N \sum_{n=0}^{\infty} R_{N,n} Z_n. \quad (19)$$

IV. CONSTANT WAKE

Several realistic examples of the wake will be considered in Sec. V. However, the simplest model of constant wake $w = 1$, $q = q_0$ is preliminary investigated in this section to discover the main features of the effect. Though the wakes are negative in the most cases [2], the positive wake is possible as well and it was observed in practice [10, 11]. Therefore both signs of the parameter q_0 are analyzed in the section.

It is easy to verify that, at $w = 1$ and $N \neq 0$, the matrix $R_{N,n}$ is

$$R_{N,n} = -\frac{\delta_{N-1,n}}{(2N-1)(2N+1)} + \frac{\delta_{N+1,n}}{(2N+1)(2N+3)}. \quad (20)$$

(its small fragment is shown in Table I).

One can check as well that $\nu_{0,0} = 0$, $S_{0,0} = 1$, that is $W_0 = 1/\nu$. Using these features, one can represent the solvability condition of series (19), that is the dispersion equation for the bunch eigentunes, in terms of an infinite continued fraction

$$\nu - q_0 + \frac{(q_0/3)^2 W_1}{1 + \frac{(q_0/15)^2 W_1 W_2}{1 + \frac{(q_0/35)^2 W_2 W_3}{1 + \dots}}} = 0. \quad (21)$$

TABLE I: Fragment of the matrix $R_{N,n}$. Its general form is given by Eq. (13) and (16).

$n \rightarrow$	0	1	2	3	4	5
$N = 0$	1	1/3	0	0	0	0
$N = 1$	-1/3	0	1/15	0	0	0
$N = 2$	0	-1/15	0	1/35	0	0
$N = 3$	0	0	-1/35	0	1/63	0
$N = 4$	0	0	0	-1/63	0	1/99
$N = 5$	0	0	0	0	-1/99	0

This expression has to be truncated in reality by applying of the assumption $W_n = 0$ at $n \geq n_{\max}$. Assigning the truncated left-hand part of Eq. (21) as $T_{n_{\max}}(\nu)$, one can write the approximate dispersion equation as

$$T_{n_{\max}}(\nu) = 0 \quad (22)$$

with the following recurrent relations:

$$T_n = T_{n-1} + T_{n-2} \frac{q_0^2 W_{n-1} W_n}{(4n^2 - 1)^2}, \quad (n \geq 2) \quad (23)$$

and the boundary conditions:

$$T_0 = \nu - q_0, \quad (24a)$$

$$T_1 = \nu - q_0 + \left(\frac{q_0}{3}\right)^2 \frac{3(\nu + \Delta Q)}{\nu(\nu + \Delta Q) - Q_s^2}. \quad (24b)$$

A. Three-mode approximation

Equation (22) is trivial at $n_{\max} = 0$: $T_0(\nu) = 0$ that is $\nu = q_0$, as it follows from Eq. (24a). It describes the wake contribution to the tune of the lowest (rigid) head-tail mode of the bunch. Of course, the TMCI cannot appear in this approximation, and the simplest equation to disclose it is $T_1(\nu) = 0$ that is, in accordance with Eq. (24b)

$$(\nu - q) \left(\nu - \frac{Q_s^2}{\nu + \Delta Q} \right) = -\frac{q_0^2}{3}. \quad (25)$$

This third order equation exactly coincides with Eq. (7.3) of Ref. [7] (without chromaticity) despite the fact that the very different concepts have been used to derive them. However, the examples presented in [7] have been restricted by the modest SC tune shift: $\Delta Q/Q_s < 3$. The situation beyond this region will be explored here for the best understanding of the phenomenon, and for further development of the techniques.

Imaginary part of a solution of Eq. (25) is plotted in Fig. 3 against the wake strength at different SC. According to the plot, the instability threshold is $|q_{th}/Q_s| = 0.567$ at $\Delta Q = 0$ (the black lines). Its dependence on $\Delta Q/Q_s$ is shown in Fig. 4. The plot is very simple at $q_0 > 0$: the threshold goes down monotonically tending to 0 when the space charge increases. The case of negative wake is more complicated and requires a special comment. Absolute value of its threshold increases with ΔQ reach[nd $q_{th}/Q_s \simeq -4$ at $\Delta Q/Q_s = 3.46$ (blue parabola in Fig. 3). The picture crucially changes after that because a new region of instability arises whose initial position is shown as the blue point in Fig. 3. Then it quickly expands stepping through the green oval to the brown one and joining with the primary region of instability (brown parabola) at $\Delta Q/Q_s = 3.69$. The barrier between the parts tears at higher ΔQ resulting in a single region of instability (red). Its right-hand boundary goes to the right, that is the TMCI threshold goes down, if the SC tune shift continues to grow up.

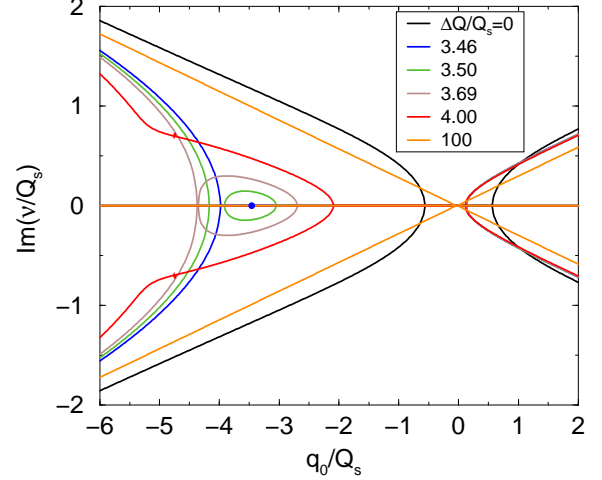


FIG. 3: Imaginary part of the boxcar eigentunes against the wake strength at different value of space charge tune shift. There are 2 regions of instability if the wake is negative and $3.46 < \Delta Q/Q_s < 3.69$.

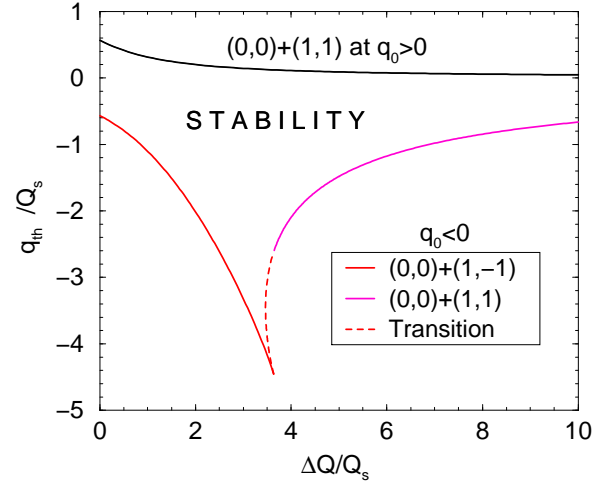


FIG. 4: Instability threshold of the boxcar bunch against SC tune shift (positive and negative wakes). Indexes of the coalesced modes are shown for each part of the threshold line.

B. Higher approximations

Higher approximations should be involved to validate the three-mode model, to establish its applicability limit, and to go beyond it.

The first step in this way is an investigation of the equation $T_2(\nu) = 0$. According to Eqs. (23) and (24), its expanded form is

$$\nu - q_0 + \frac{q_0^2 W_1(\nu)}{9} + \frac{q_0^2 (\nu - q_0) W_1(\nu) W_2(\nu)}{225} = 0 \quad (26)$$

where

$$W_1(\nu) = \frac{3(\nu + \Delta Q)}{\nu(\nu + \Delta Q) - Q_s^2}, \quad (27a)$$

$$W_2(\nu) = \frac{|S_{2,-2}|^2}{\nu - \nu_{2,-2}} + \frac{|S_{2,0}|^2}{\nu - \nu_{2,0}} + \frac{|S_{2,2}|^2}{\nu - \nu_{2,2}}. \quad (27b)$$

Required parameters have to be obtained by solution of Eq. (13) with $n = 2$ as it is described in the Appendix. With the notations $\nu_{n,m} = \hat{\nu}_{n,m}Q_s - \Delta Q$, the eigentunes appear as all roots of the dispersion equation

$$\hat{\nu}_{2,m}(\hat{\nu}_{2,m}^2 - 4) = \frac{\Delta Q}{Q_s}(\hat{\nu}_{2,m}^2 - 1), \quad (28)$$

and formula for corresponding normalizing coefficients is

$$|S_{2,m}|^2 = \frac{5(\hat{\nu}_{2,m}^2 - 1)^2}{\hat{\nu}_{2,m}^4 + \hat{\nu}_{2,m}^2 + 4}. \quad (29)$$

The substitution of the functions $W_{1-2}(\theta)$ into Eq. (26) results in the equation of 6th power

$$(\nu - q_0) \left(\nu - \frac{Q_s^2}{\nu + \Delta Q} \right) + \frac{q_0^2}{3} = -\frac{q_0^2(\nu - q)}{75} \times \left(\frac{|S_{2,-2}|^2}{\nu - \nu_{2,-2}} + \frac{|S_{2,0}|^2}{\nu - \nu_{2,0}} + \frac{|S_{2,2}|^2}{\nu - \nu_{2,2}} \right). \quad (30)$$

This equation has 6 roots which are different real numbers inside the stability area. However, at least 2 of them should be coinciding at the boundary of this area, which feature can be used for the search of the instability threshold. Corresponding threshold of negative wake is presented in Fig. 5 by the magenta line. The case $q_0 > 0$ is not considered in this subsection because the result almost does not depend on n_{max} and can be reasonably described by the three-mode approximation, Eq. (25).

Similar method can be used for analysis of higher approximations though corresponding formulae are essentially more cumbersome. Generally, the case involves $(n_{max} + 1)(n_{max} + 2)/2$ basis vectors and leads to algebraic equation of the same power, where n_{max} is order of the highest used Legendre polynomial.

Results of the calculations are collected in Fig. 5 at $n_{max} = 1 - 12$ (dispersion equation of 3 – 91 power). It is seen that, at rather small SC, absolute value of the threshold rises with ΔQ , different approximations provide actually coinciding results in their region of applicability, and each additional step simply expands this region. For example, the three-mode approximation ($n_{max} = 1$) provides correct magnitude of the threshold at $\Delta Q/Q_s \leq 3.46$ but at least $n_{max} = 12$ (91-mode approximation) is needed to get proper results within the range $\Delta Q/Q_s = 0 - 12$.

The sequential decrease of the threshold cannot be treated as a physical effect because of absence of the convergence. The opposite assumption which has been admitted in my preprint [8] was coming from an insufficient accuracy of numerical calculations which has led to an incomplete separation of numerous and very tightly spaced radial modes.

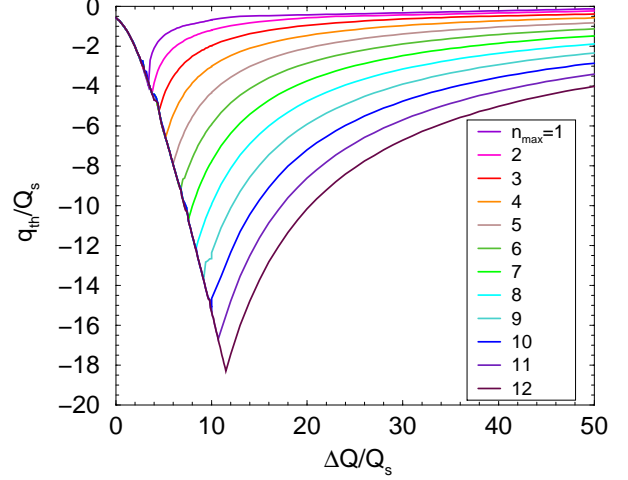


FIG. 5: Threshold curve of the boxcar bunch in different approximations. Index n_{max} means maximal power of the Legendre polynomial in the expansion.

C. The bunch spectrum

The inadequate convergence of the curves in Fig. 5 remains the open question: which is the TMCI threshold of negative wake at very large magnitude of $\Delta Q/Q_s$, such as several tens or more? There is a related information in Ref. [6]: at such conditions, the TMCI cannot be caused by a coalescence of positive eigentunes of the bunch. The last reservation is important because only a part of the boxcar modes has been used for the analysis in [6]. Tunes of these modes are located in the upper part of Fig. 1. Therefore, more detailed examination of the bunch spectrum is needed with the wake to check the results, including all bunch tunes $\nu_{th}(\Delta Q)$ at the frontier of the TMCI area.

Very first example of this has been given in Fig. 4 where indexes of the coalesced modes are specified for the three-mode approximation. The more detailed view is represented in Fig. 6 where full spectrum of the bunch is plotted at $n_{max} = 5$ (21-mode approximation). The most important spectral lines are displayed by special colors: blue for the modes $\{0,0\}$ and $\{1,-1\}$, and red for the modes $\{5,5\}$ and $\{4,4\}$. According to the picture, the coalescence of these modes is responsible for the TMCI at $\Delta Q/Q_s < 6$ or > 6 , correspondingly. Just the switching from the lower pair to the upper one causes the sharp kink of the threshold curve which is shown in the plot by dashed line. An incidental interference of other modes slightly affects the curve but does not change its general contour.

Another examples are given in Fig. 7 where the most important spectral lines are plotted at three different approximations with $n_{max} = 6, 9, 12$. The lower curves represent tunes of the modes $\{0,0\} + \{1,-1\}$ which are coalesced in the beginning and are closely located later.

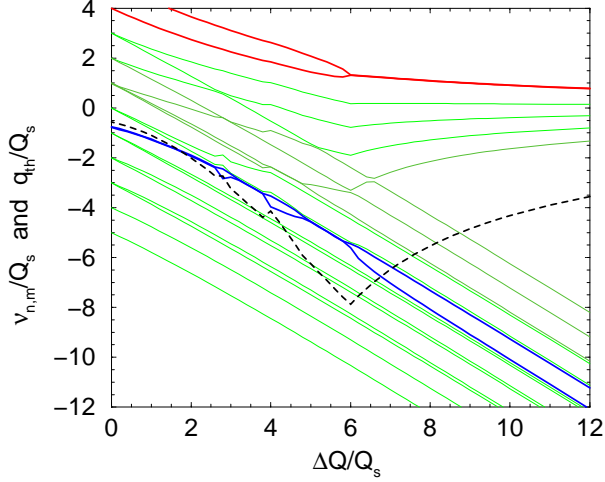


FIG. 6: The bunch spectrum in the TMCI frontier at $n_{\max} = 5$ (21-mode approximation). The most important modes are shown by blue and red lines. The TMCI threshold is represented by the dashed black line.

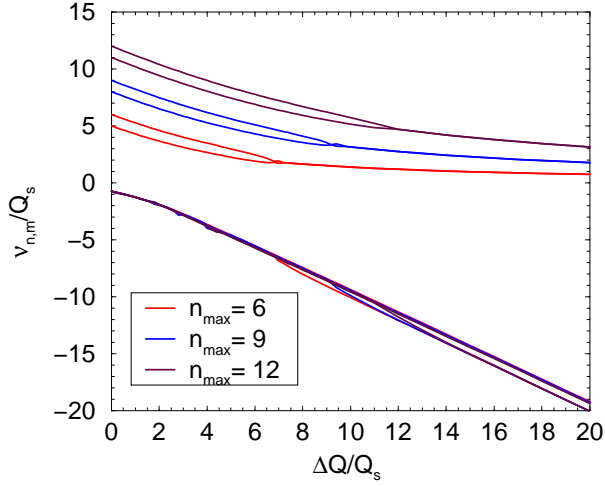


FIG. 7: The most important spectral lines in different approximations. The lower lines: modes $\{0,0\}$ and $\{1,-1\}$; the upper ones: the highest observed tunes in given approximation.

The convergence manifests itself in the fact that the coalesced part of the curves expands when n_{\max} increases. The upper curves in Fig. 7 represent the tunes

$$\{n_{\max}, n_{\max}\} + \{n_{\max} - 1, n_{\max} - 1\}$$

It is seen that the lines of the same color merge at rather large $\Delta Q/Q_s$. However, it is a divergent process because the junction point does not tend to a certain limit when n_{\max} increases. It inevitably leads to the conclusion that the junction of the positive tunes in Figs. 6 and 7, as well as the associated leap of the threshold, are not a physical

effects. The engaging of Ref. [6] allow to assert that this statement should be true in any approximation

Therefore a monotonous rising of the TMCI threshold looks as the most credible assumption. It also compliance with behavior of the low crucial modes which are

$$\nu_{0,0} \sim q_0, \quad \nu_{1,-1} \simeq -Q_s - \Delta Q.$$

According this, the instability condition $\nu_{0,0} = \nu_{1,-1}$ should result in the threshold relation $q_{th} \sim -\Delta Q$.

V. TMCI WITH REALISTIC WAKE

Series of equations (19) with matrix $R_{N,n}$ given by Eq. (15) is applicable at any wake function $q(\theta) = q_0 w(\theta)$. However, dispersion equation (21) and its approximate forms provided by Eqs. (22)-(24) are valid only with constant wake. Therefore, more standard procedures should be generally used for solution of Eq. (19). It results in some deterioration of the accuracy and compels to restrict number of used basis vectors. Performed calculations with constant wake attest that the “old” and the “new” results coincide at $n_{\max} \leq 9$ (55-modes approximation), otherwise some real roots can be lost. This restriction is accepted below at the calculations with realistic wakes.

A. Resistive wall wake

Resistive wall impedance is the most general and important source of transverse instabilities in circular accelerators. At $z \gg \lambda$, its wake function is [2]:

$$W_1(z) = -\frac{4R}{b^3} \sqrt{\frac{c}{\sigma z}} \quad (31)$$

where b is the beam pipe radius, σ is the pipe wall conductivity, and z is distance from the field source to the observation point. Taking into account Eqs. 5 and (17), one can write the normalized wake function as $q = q_0 w(\theta)$ with

$$q_0 = -\frac{4r_0 R^2 N_b}{3\pi\gamma\beta b^3 Q_0} \sqrt{\frac{c}{\sigma z_b}}, \quad w(\theta) = \frac{3}{4\sqrt{2}\theta} \quad (32)$$

TABLE II: Fragment of the matrix $R_{N,n}$ for resistive wake.

$n \rightarrow$	0	1	2	3	4	5
$N = 0$	1	.20000	-.02857	.00952	-.00433	.00233
$N = 1$	-.20000	.14286	.06667	-.01299	.00513	-.00260
$N = 2$	-.02857	-.06667	.06494	.03590	.00779	.00332
$N = 3$	-.00952	-.01299	-.03590	.03896	.02323	-.00533
$N = 4$	-.00433	-.00513	-.00779	-.02323	.02666	.01659
$N = 5$	-.00233	-.00260	-.00332	-.00533	-.01659	.01970

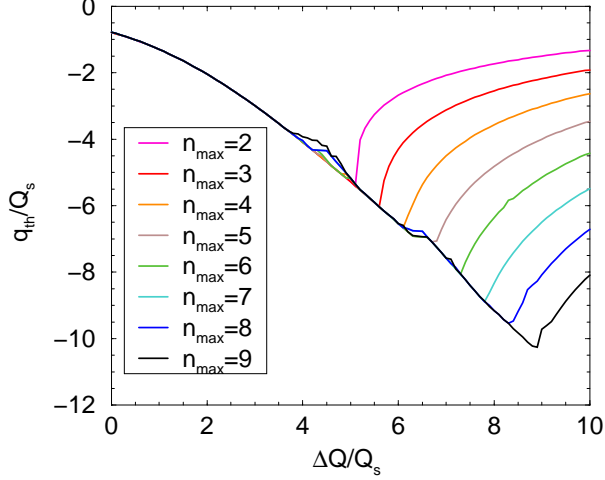


FIG. 8: Stability region of the boxcar bunch with resistive wall wake. Normalized magnitude of the wake is given by Eq. (32), index n_{\max} means maximal power of Legendre polynomial in the expansion.

where z_b is the bunch length in usual units. Generally speaking, this wake can cause multiturn collective effects as well. However, their influence on the TMCI threshold is negligible for a single bunch with $z_b \ll 2\pi R$ [7] which assumption is used further. Then series (19) is applicable with the matrix $R_{N,n}$ whose part is represented in Table II. Threshold of this instability is plotted in different approximations in Fig. 8. which is very similar to Fig. 5 (constant wake) both in the form and in the magnitude.

B. Short square wake

A square wake can be created by a strip-line BPM or by a traveling-wave kicker [2]. The long (constant) square wake is considered above in detail. However, the wake can be shorter than the bunch, in practice. In accordance with Eq. (17), its normalized strength should be represented in the form

$$q(\theta) = q_0 w(\theta) = \frac{4q_0}{\theta_w(4 - \theta_w)} \quad \text{at } 0 < \theta < \theta_w \quad (33)$$

where $\theta_w < 2$ is the wake length (recall that the bunch length is 2 in these units). Several examples are represented in Fig. 9 at $n_{\max} = 9$. Note that the horizontal lines have no physical sense and are added to mark end of the curve applicability (the calculations were not carried out after that). Due to the normalization, the threshold dependence on the SC tune shift is not very significant, especially at $\Delta Q/Q_s < 5$.

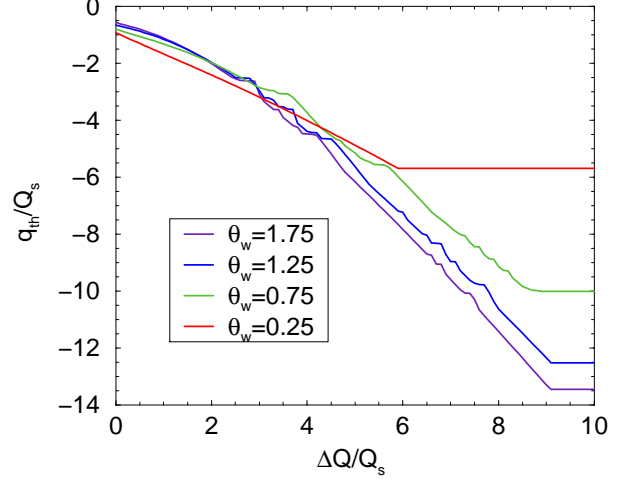


FIG. 9: TMCI threshold of short square wake against SC tune shift. Length of the wake is θ_w , the bunch length=2. The approximation with $n_{\max} = 9$ (55 modes) is used, the horizontal lines mark end of the applicability area.

C. Oscillating wake

There are several models considering the wake field source as a resonator of frequency $f = c/\lambda$ [2]. It creates an oscillating wake $\propto \cos(2\pi z/\lambda)$ having the phase advance $\phi = 2\pi z_b/\lambda$ within the bunch. We consider the case $\phi < 2\pi$, and represent the wake in the form satisfying the normalization condition (17):

$$q(\theta) = q_0 w(\theta), \quad w(\theta) = \frac{\phi^2 \cos(\phi\theta/2)}{2(1 - \cos\phi)} \quad (34)$$

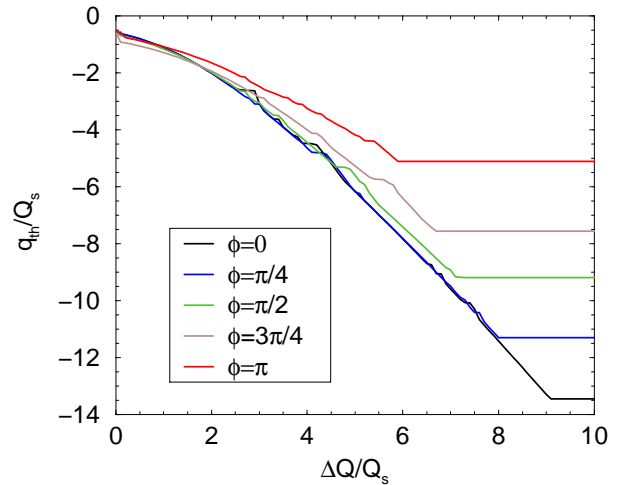


FIG. 10: TMCI threshold of oscillating wake with phase advance ϕ within the bunch of length $\Delta\theta = 2$. $n_{\max} = 7$ (36-mode approximation).

Several examples are represented in Fig. 10 at $n_{max} = 7$ to demonstrate that SC produces a stabilizing effect in these cases as well.

VI. CONCLUSION

Being stable in themselves, the eigenmodes of the box-car bunch with space charge form a convenient and effective basis for investigation of the bunch instability with the space charge and a wake field. The dispersion equation derived by this method at the constant wake is represented in the form of an infinite continued fraction as well as in the form of a recursive relation with arbitrary number of the basis functions involved.

It is shown that the TMCI threshold of the negative constant wake grows up in absolute value when the SC tune shift increases. An enlargement of number of the used basis vectors expands area of applicability of this statement but does not change the results obtained before. The statement is confirmed in the paper by the straightforward calculation of the threshold at $\Delta Q/Q_s \leq 12$ using the basis set including up to 91 eigenfunctions. Convergence of the solutions is not achieved at higher SC because very large number of the eigenfunctions is required for separation of different radial modes. However, an additional analysis of the bunch spectrum allows to extend the statement to any tune shift.

Similar results are obtained with realistic wake functions including the resistive wall, the short square, and the oscillating forms.

Threshold of the positive wake goes down when the SC tune shift increases, and the effect can be satisfactory described by the three-mode approximation.

VII. ACKNOWLEDGMENTS

FNAL is operated by Fermi Research Alliance, LLC under contract No. DE-AC02-07CH11395 with the United States Department of Energy.

VIII. APPENDIX

Using the notation

$$\hat{\nu}_{n,m} = \frac{\nu_{n,m} + \Delta Q}{Q_s}, \quad \hat{\Delta Q} = \frac{\Delta Q}{Q_s}, \quad P_n(\theta) = \sum_{l=0}^n p_{nl} \theta^l \quad (A1)$$

one can rewrite Eq. (13) in the form

$$\hat{\nu}_{n,m} Y_{n,m} + i \frac{\partial Y_{n,m}}{\partial \phi} = S_{n,m} \hat{\Delta Q} \sum_{l=0}^n p_{n,l} (A \cos \phi)^l \quad (A2)$$

Its solution is

$$Y_{n,m} = S_{n,m} \hat{\Delta Q} \sum_{k=-n}^n \frac{\exp i k \phi}{\hat{\nu}_{n,m} - k} \sum_{j=0}^n U_{n,k,j} A^{k+2j} \quad (A3)$$

where

$$U_{n,k,j} = \frac{p_{n,k+2j}}{2^{k+2j}} \binom{k+2j}{j} \times \begin{cases} 1 & \text{at } k+j \geq 0 \\ 0 & \text{at } k+j < 0 \end{cases} \quad (A4)$$

This function should satisfy normalization condition represented by Eq. (7) with $j \equiv \{n, m\}$ and distribution function (11a). The substitution results in the relation:

$$\frac{1}{S_{n,m}^2 \Delta \hat{Q}^2} = \sum_{k=-n}^n \frac{1}{(\hat{\nu}_{n,m} - k)^2} \times \sum_{j_1=0}^n \sum_{j_2=0}^n U_{n,k,j_1} U_{n,k,j_2} \overline{A^{2(k+j_1+j_2)}} \quad (A5)$$

where $\overline{A^{2j}}$ is the amplitude power averaged over the distribution:

$$\overline{A^{2j}} = \int_0^1 \frac{A^{2j+1} dA}{\sqrt{1-A^2}} = \sum_{l=0}^j \binom{j}{l} \frac{(-1)^l}{2l+1} \quad (A6)$$

In principle, involved eigentunes $\nu_{n,m}$ could be obtained by substitution of Eq. (A3) into Eq. (4) with the functions Y and \bar{Y} being taken from this Appendix. Because similar calculation has been actually accomplished in Ref. [9], we represent here only the resulting equation for the eigentunes:

Lower powers

$$\hat{\nu}_{0,0} = \hat{\Delta Q}, \quad \hat{\nu}_{1,\pm 1}^2 - 1 = \hat{\Delta Q} \hat{\nu}_{1,\pm 1} \quad (A7)$$

Higher even powers

$$\begin{aligned} & \hat{\nu}_{n,m} [\hat{\nu}_{n,m}^2 - 4] \dots [\hat{\nu}_{n,m}^2 - n^2] \\ &= \hat{\Delta Q} [\hat{\nu}_{n,m}^2 - 1] \dots [\hat{\nu}_{n,m}^2 - (n-1)^2] \end{aligned} \quad (A8)$$

Higher odd powers

$$\begin{aligned} & [\hat{\nu}_{n,m}^2 - 1] \dots [\hat{\nu}_{n,m}^2 - n^2] \\ &= \hat{\Delta Q} \hat{\nu}_{n,m} [\hat{\nu}_{n,m}^2 - 4] \dots [\hat{\nu}_{n,m}^2 - (n-1)^2] \end{aligned} \quad (A9)$$

Some of the values $\nu_{n,m}/Q_s = \hat{\nu}_{n,m} - \hat{\Delta Q}$ are plotted in Fig. 1. Factors $S_{n,m}^2$ can be found from Eq. (A5) with the known eigentunes substituted. Some results are represented below:

$$S_{0,0}^2 = 1, \quad S_{1,\pm 1}^2 = \frac{3\hat{\nu}_{1,\pm 1}^2}{\hat{\nu}_{1,\pm 1}^2 + 1}, \quad (A10)$$

$$S_{2,m}^2 = \frac{5(\hat{\nu}_{2,m} - 1)^2}{\hat{\nu}_{2,m}^4 + \hat{\nu}_{2,m}^2 + 4}, \quad m = 2, 0, -2, \quad (A11)$$

$$S_{3,m}^2 = \frac{7\hat{\nu}_{3,m}^2(\hat{\nu}_{3,m}^2 - 4)^2}{\hat{\nu}_{3,m}^6 - 2\hat{\nu}_{3,m}^4 + 13\hat{\nu}_{3,m}^2 + 36}, \quad (A12)$$

etc.

-
- [1] R. Kohaupt, in *Proceeding of the XI International Particle Accelerator Conference*, p.562, Geneva, Switzerland, (1980). DESY Rep. M-80/19 (1980).
 - [2] K. Y. Ng, “Physics of Intensity Dependent Beam Instabilities”, Fermilab-FN-07-13 (2002).
 - [3] M. Blaskiewicz, Phys. Rev. ST Accel. Beams 1, 044201 (1998).
 - [4] M. Blaskiewicz, in *Proceeding of International Particle Accelerator Conference (IPAC2012)*, May 20-25, New Orleans, USA, 2012, p. 3165.
 - [5] A. Burov, Phys. Rev. ST Accel. Beams 12,044202 (2009).
 - [6] V. Balbekov, Phys. Rev. ST Accel. Beams 14, 094401 (2011).
 - [7] V. Balbekov, JINST 10 P10032 (2015).
 - [8] V. Balbekov, FERMILAB-PUB-16-079-APC (2016).
 - [9] F. Sacherer, CERN Rep. SI-BR-72-5 (1972).
 - [10] H. G. Hereward, CERN Rep. MPS-Int-DL-64-8 (1964).
 - [11] V. I. Balbekov, K. F. Gertsev, At.Energ.41 p.408 (1975). (DOI: 10.1007/BF01119511).